SAND2019-15226J

Interfacial Toughness: Dependence on Surface Roughness and Test Temperature

E. D. Reedy, Jr.*and M. E. Stavig
Sandia National Laboratories
Albuquerque, NM, USA
edreedy@sandia.gov

Abstract

Interfacial toughness quantifies resistance to crack growth along an interface and in this investigation the toughness of an aluminum/epoxy interface was measured as a function of surface roughness and test temperature. The large strain response of the relatively ductile epoxy adhesive used in this study was also characterized. This epoxy adhesive exhibits intrinsic strain-softening after initial compressive yield and then deforms plastically at a roughly constant flow stress until it rapidly hardens at large compressive strains. We find that interface toughness scales as the product of the temperature dependent epoxy yield strength and a length scale that characterizes surface roughness. The proposed scaling is based upon dimensional considerations of a model problem that assumes that the characteristic length scale of both the roughness and the crack-tip yield zone is small relative to the region dominated by the linear elastic asymptotic crack-tip stress field. Furthermore, the model assumes that interfacial failure occurs only after the epoxy begins to harden at large strains. The proposed relationship is validated by our interfacial toughness measurements.

1 Introduction

The performance and reliability of many mechanical and electrical components depend on the integrity of polymer-solid interfaces. Interfacial toughness Γ characterizes the energy to propagate an existing interfacial crack. In the present study only the case where the extent of crack-tip yielding is small compared to all geometric length scales is considered. Interfacial toughness can be regarded to be a material property under such conditions. As such it can be used as a measure of bond quality as well as a primary input in finite element simulations of crack growth in adhesively bonded and encapsulated structures. Interfacial toughness depends on many variables including test temperature, rate of loading, surface roughness, and interfacial chemistry. It also depends on the level of crack-tip energy dissipation (e.g., yielding) that occurs in the adjacent bulk materials. The relationship between toughness values and the parameters that control toughness is in general unknown and must be determined through extensive testing.

There are numerous methods for measuring interfacial toughness (Hutchinson and Suo 1992, Volinsky, Moody et al. 2002). In this study, an adhesively bonded, asymmetric double cantilever beam (ADCB) specimen was used (Brown 1990). One aspect of interfacial fracture mechanics that distinguishes it from traditional linear elastic fracture mechanics is the role of crack-tip mode-mixity (Hutchinson and Suo 1992). Geometric and material asymmetries with respect to the interface are responsible for the inherently mixed-mode condition found at the tip of an interfacial crack. Even for a symmetric loading, elastic asymmetry generates both normal and shear stress on the interface ahead of the crack tip and the ratio of these stresses changes with distance from the crack tip. The level of mode-mixity $\psi_{r=l}$ (defined as the arctangent of the ratio of the shear stress to normal stress at a fixed distance l in front of the crack tip in the region dominated by the stress singularity) depends on the mismatch in elastic properties as well as specimen geometry and loading. Mode-mixity is important because the value of the interfacial toughness can be highly dependent on the level of mode-mixity. The ADCB specimen design used in this study produces a predominantly Mode I-like loading near the crack-tip with a slight tendency to push the crack towards the interface so as to keep it on the interface. One virtue of the ADCB specimen is that the interfacial crack propagates stably under increasing applied load-point displacement so that multiple toughness measurements can be made using a single sample.

It is well known that measured joint strength can increase with increasing surface roughness (Jennings 1972, Shahid and Hashim 2002). For example, there is a 40-80% increase in strength of adhesively bonded, cylindrical butt joints when the root mean square surface roughness of the aluminum adherends is increased from 1 to 5 micrometers (Reedy and Guess 1999). These tests were performed at room temperature (far below the adhesive's glass transition temperature T_g) and in all of the tests failure initiated at the interface along a segment of the specimen periphery. Others have reported an increase in measured interfacial toughness with increasing surface roughness (Zhang and Spinks 1997, Rider and Arnott 2001, Zhang, Panat et al. 2003). An increase in joint strength with increasing surface roughness has been attributed to a number of factors including an increase in the real interfacial surface area, enhanced plastic energy dissipation in the bulk materials, crack deflection, and mechanical interlock (Kinloch 1980, Pocius 1997, Packham 2003). The strength of adhesively bonded joints can also vary with test temperature although the trend is not as well established. For example, adhesively bonded tensile-loaded single lap joints seem to show either an increase or a decrease in strength that depends on the type of adhesive used (Kinloch 1982). Other work has reported that the strength of adhesively bonded butt joints increases with decreasing temperature when the joints are tested well below their T_g (Jennings 1972, Reedy and Guess 1995).

The adhesive's bulk properties will also influence the measured interfacial toughness since crack-tip energy dissipation by way of adhesive yielding can contribute a large fraction of the measured toughness. In this study we are focused on adhesively bonded joints where the adhesive is a relatively ductile epoxy and test temperatures are well below the epoxy's T_g. Consequently, the epoxy adhesive is in a glassy state. When tested in its glassy state, this particular type of epoxy adhesive can sustain large compressive strains and often exhibits intrinsic strain-softening after initial compressive yield (i.e., there is a load drop after initial yield) (Reedy and Guess 1993, Adolf, Chambers et al. 2004). Furthermore, this softening can be followed by subsequent hardening at large compressive strains (e.g., at compressive strains >50%) (Buckley, Harding et al. 2001). Such strain softening ductile epoxies can exhibit strain localization that appears similar to the Luder's bands generated in annealed mild steel where plastic flow occurs in bands (McClintock and Argon 1966). Ductile epoxies are thought to be lightly cross-linked thermosetting materials and this sort of epoxy is known to promote significant shear banding in rubber toughened epoxies (tightly cross-

linked structures are not toughenable) (Bagheri, Marouf et al. 2009). Coarse-grained molecular dynamics simulations of a cross-linked epoxy network bonded to a solid interface also predict a stress-strain curve where intrinsic strain-softening occurs (Stevens 2001). The predicted softening is followed by a plateau region of roughly constant stress that is in turn followed by a region of rapid hardening at large strains. In these calculations the polymer strands between cross-links are not initially taut, and they become taut only after relatively high average network strains. Once the strands are taut, the simulation predicts that the molecular bonds begin to stretch, and stress rises rapidly as the epoxy hardens. Predicted interfacial bond failures occur only after the polymer strands between cross-links are pulled taut and the epoxy is hardening.

Reported below are results of a study that investigated how surface roughness and test temperature impact the measured toughness of an aluminum/epoxy interface. Note that all test temperatures were well below the epoxy's T_g and consequently the epoxy was in a glassy state at all test temperatures. Accordingly, under such circumstances it is reasonable to idealize the epoxy as an elastic-plastic material with a temperature dependent yield strength. Viscoelastic response is not considered in this work and the results presented here are not expected to apply when test temperatures approach the epoxy's T_g. In the following, the experimental results are presented first, and then a model that elucidates the connection between interfacial toughness, surface roughness, and test temperature is presented next. This model suggests a simple connection between the quantities of interest, and the proposed scaling relationship is in good agreement with the measured temperature and surface roughness dependent toughness values.

2 Experiment

2.1 Materials

Two different epoxy adhesives were used in this study. Most specimens were fabricated using a diglycidyl ether of bisphenol A (EPON® Resin 828) resin cured with diethanolamine (DEA) at a 100:12 parts by weight mix ratio. This epoxy is referred to as EPON 828/DEA and as cured has a glass transition temperature of T_g of 70° C. Other samples were fabricated using an EPON® Resin 828 cured with polyetheramine (Jeffamine® T-403) at a 100:43 parts by weight mix ratio. This epoxy is referred to as EPON 828/T403 and as cured has a T_g of 85° C. Table 1 lists the temperature

dependent Young's modulus E and yield strength σ_y for both epoxies when tested in compression at a nominal strain rate of 0.001/s (tested molded epoxy cylinders with a length/diameter ratio of ≈ 2 in compression). The samples were tested at room temperature (RT), -20° C, or -60°C. Note that there is essentially a linear variation in the measured yield strength with test temperature (Fig. 1), so one can readily relate test temperature to epoxy yield strength.

Table 1. Temperature-dependent compressive Young's modulus E and yield strength σ_y for the two epoxy adhesives used in this study.

	EPON 828/DEA T_g=70 °C		EPON 828/T403 T_g=85 °C	
T (C)	E (GPa)	σ_y (MPa)	E (GPa)	σ_y (MPa)
RT	2.7	94	2.9	88
-20	3.0	129	3.1	131
-60	3.6	176	3.8	180

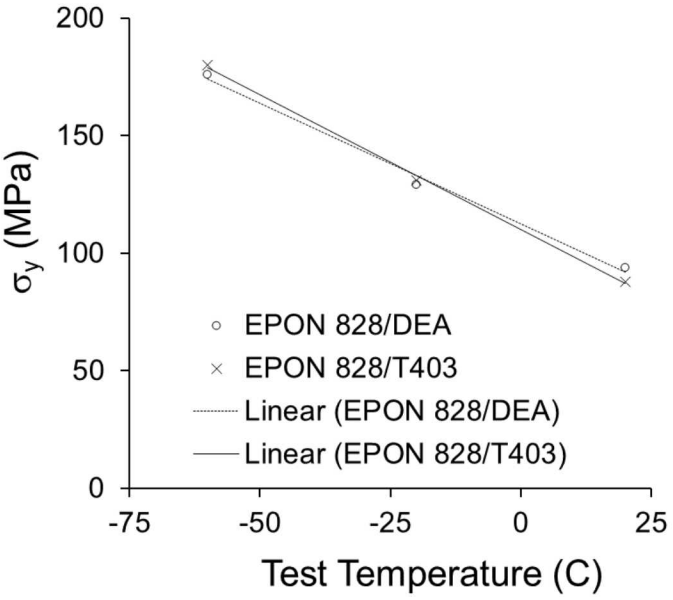

Figure 1. Variation of yield strength σ_y with test temperature for the two epoxy adhesives used in this study.

2.2 Test procedures

2.2.1 Large deformation epoxy compression tests

The aim of these tests was to investigate the large strain response of the epoxy adhesives used in this study. Compression tests were performed since epoxy adhesives typically fail at low strains when tested in tension (presumably because of their relatively low fracture toughness and the presence of small surface flaws). To ensure that initial yielding occurs at a known position, a cylindrical specimen with a reduced mid-plane cross-section was used. The specimen has a nominal 16 mm diameter that gradually tapers over a 25 mm long central section of the 38 mm long specimen to a 14.4 mm minimum diameter (i.e., tapered to 90% of nominal diameter with taper defined by a segment of a circular arc). The specimen was bonded to the platens of a subpress to keep the specimen from shifting. Since the sample is waisted, there is limited yielding at the platens during the test. Samples were soaked at the test temperature for a time sufficient to uniformly cool the sample. An extensometer was used to measure the axial deformation over a 12.7 mm gage length in some tests, while in other tests the change in diameter at the reduced-section mid-plane was measured. The cross-head displacement and applied load was measured in all tests. The load vs diameter data was used to determine true stress. The axial displacement about the waist's central 12.7 mm gage length was used to get an approximate measure of true axial compressive strain (ln(1 + measured axial strain)). This approximate measure of true axial compressive strain is used since the epoxy that was tested can strain soften and strain softening leads to localized deformation and nonuniform strain within the gage section. True stress and strain were correlated through their common measurement of the sample's nominal axial strain as determined by cross-head displacement.

2.2.2 Interfacial toughness tests

Interfacial fracture toughness quantifies the resistance to crack growth along an interface. The aluminum/epoxy interfaces studied in this work are relatively brittle with estimated plastic zone sizes that are small compared to bond thickness (specific results for plastic zone size are presented later in Section 3). Consequently, the measured toughness can be considered to be a material property. In this study, an adhesively bonded, asymmetric double cantilever beam (ADCB) specimen was used to measure interfacial toughness (Fig. 2). The ADCB specimen used in this

study bonds 4.7 and 8.9 mm thick 6061-T6 aluminum beams together with a nominally 0.5 mm-thick epoxy layer. Both beams are 12.7 mm wide and 120 mm long. Small spacers are bonded to the ends of one of the adherends to define the epoxy layer thickness and the edges of the specimen are sealed with Teflon tape to form a cavity that is to be filled with epoxy. The cavity is filled by injecting epoxy through a small hole in one end of the thicker beam and allowing the epoxy to flow along the entire length of the cavity and then out of a small hole on the opposing end of the beam.

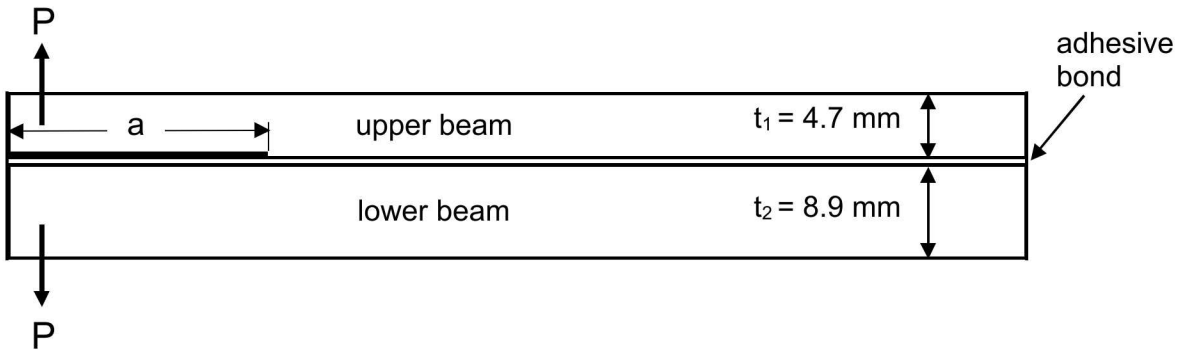

Figure 2. Adhesively bonded, asymmetric double cantilever beam (ADCB) specimen.

The ADCB specimen is pinned into a load train that utilizes a chain linkage and is loaded by pulling the ends apart at a crosshead displacement rate of 0.02 mm/s to propagate a crack along the interface with the thinner beam. The crack grows stably with increasing end displacement allowing several toughness measurements to be made while testing a single specimen. Crack length is inferred from specimen compliance, and the specimen is unloaded and reloaded during the test to establish the crack length during the loading step. The calibration used to determine toughness values from the inferred crack length and the load at the initiation of crack growth is based on published results for a homogeneous asymmetrical double cantilever beam specimen that ignores the compliance of the thin adhesive bond (Bao, Ho et al. 1992). These results for a homogeneous specimen can be converted to those applicable to a sandwich test specimen with a middle layer that is thin relative to other dimensions (Suo and Hutchinson 1989). Using this conversion, the sandwich specimen employed in this study has a crack-tip mode-mixity $\psi_{r=0.01\text{ mm}}$ of about -20°. Finite element results for a similar specimen geometry that includes 0.5 mm adhesive bond layer are in reasonable agreement with a calculated $\psi_{r=0.01\text{ mm}}$ of about -15°.

The interface that was tested was either highly polished (with a measured root mean square surface roughness $R_q \approx 0.1$ μm), slightly roughened using a Scotch-Brite™ pad ($R_q \approx 1$ μm), or grit blasted ($R_q \approx$ 5-6 μm) where a 2.5 mm cutoff length was used in the surface roughness measurement. Samples were tested at room temperature (RT), -20°C, or -60°C after they were soaked at the test temperature for a time sufficient to uniformly cool a sample.

2.3 Test results

2.3.1 Epoxy stress-strain to large strains

Figure 3 plots the measured large strain compression data (true stress vs. an approximate measure of true axial compressive strain (ln(1 + measured axial strain) is plotted). The general features of the data include an initial yield point, strain-softening, a lower stress plateau, and finally hardening at large strain (the tests were terminated at a strain level of strain ≈ 0.5). Both epoxy formulations show similar response but differ in detail. Plastic deformation occurs at a roughly constant flow stress after initial post yield softening. The value of the initial yield strength as well as the flow stress is highly dependent on the test temperature. Rapid strain hardening begins at a strain level > 0.4, and this strain level is not strongly dependent on test temperature. A substantial amount of

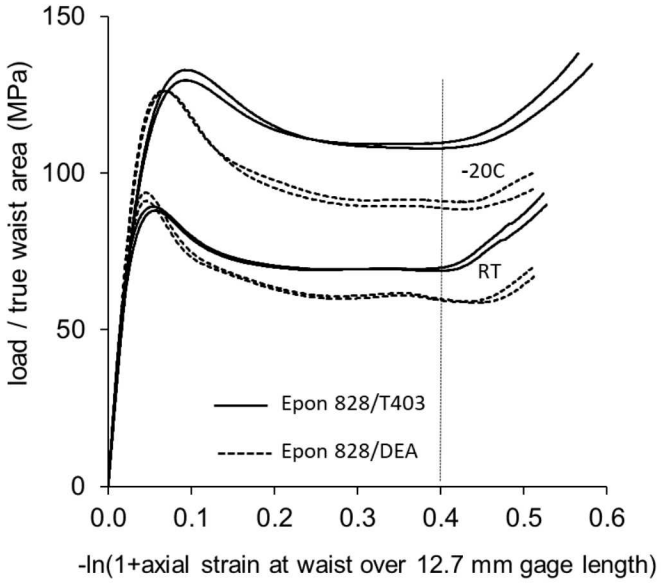

Figure 3. Large strain compression data for two epoxy adhesives.

energy dissipation can occur after initial yield and prior to hardening at high strain. Note that softening generates localized deformation, so the reported results depend on specimen geometry and loading. During loading, the specimen first begins to bulge at its midplane with the bulge's diameter and axial length increasing with load. Although details, like the precise nature of the initial softening curve, are expected to be highly dependent on specimen and measurement particulars, the overall shape of the stress-strain curve, the initial yield strength, the post yield stress plateau, and the strain at which final strain hardening occurs should reflect the actual material response.

2.3.2 Interfacial toughness data

Results for the EPON 828/DEA epoxy-to-aluminum interface are presented first (Table 2). For a fixed value of surface roughness R_q, there is at least a 45% increase in interfacial toughness Γ when the test temperature is decreased from RT to -60° C. Thus, although colder test temperatures are often associated with increased material brittleness, that is not the case for the tested interfaces. For a fixed value of test temperature T, there is at least a factor of 12 increase in Γ when R_q is increased from 0.1 μm to 6 μm. Recall that there is an essentially a linear relationship between the measured compressive yield strength and test temperature when the epoxy is tested well below its T_g (Fig. 1). Since the temperature-dependent yield strength is a basic material property, we elect to plot interfacial toughness Γ vs. epoxy yield strength in Fig. 4. Toughness varies approximately linearly with σ_y when R_q is fixed. Figure 5 shows that Γ varies approximately linearly with roughness R_q when σ_y is fixed.

Table 2. Measured EPON 828/DEA epoxy-to-aluminum interfacial toughness.

T (°C)	σ_y (MPa)	R_q (μm)	$\sigma_y R_q$ (N/mm)	Γ (J/m^2)	St Dev Γ (J/m^2)	# data pts
23	94	0.1	0.01	7.3	0.6	7
23	94	1	0.09	20.5	1.4	7
23	94	6	0.56	94	4.3	5
-20	129	0.1	0.01	7.9	0.7	8
-20	129	1	0.13	20.1	1.0	10
-20	129	6	0.77	117.6	1.4	5
-60	176	0.1	0.02	11.1	1.3	14
-60	176	1	0.18	29.8	3.1	10
-60	176	6	1.06	157.7	10.3	15

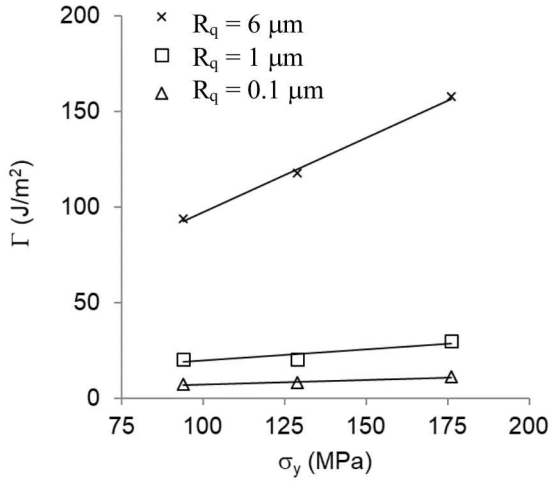

Figure 4. Measured aluminum/EPON 828/DEA epoxy interfacial toughness versus temperature dependent epoxy yield strength.

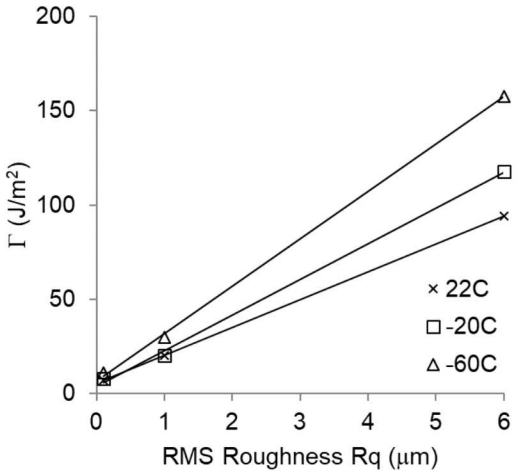

Figure 5. Measured aluminum/EPON 828/DEA epoxy interfacial toughness versus root mean square surface roughness R_q.

Energy dispersive X-Ray spectroscopy (EDS) was used to characterize the fracture surfaces and in all cases the failure was primarily interfacial. There was <1% carbon on the aluminum side of the specimens with R_q <0.1 μm (4 specimens, analyzed - 3 regions/specimen). There was ≈ 2-6%

carbon on the aluminum side of the specimens with R_q ≈1.0 μm (2 specimens analyzed - 3 regions/specimen). The grit blasted surfaces with R_q ≈ 6.0 μm had ≈ 7-8% carbon on aluminum fracture surface (2 specimens analyzed - 3 regions/specimen). Here isolated patches of epoxy appear to be left behind within deep crevices as the crack propagates across these features.

Results from a more limited study of an EPON 828/T403 epoxy-to-aluminum interface show a similar dependence on temperature and interfacial roughness (Table 3). There is an 80% increase in Γ when the test temperature is decreased from RT to -65° C (R_q = 4 μm). There is factor of 8 increase in Γ when R_q is increased from 0.1 μm to 5 μm (tested at RT). Toughness varies approximately linearly with σ_y when R_q is fixed (Fig. 6) and Γ varies approximately linearly with roughness R_q when σ_y is fixed (Fig. 7).

Table 3. Measured EPON 828/T403 epoxy-to-aluminum interfacial toughness.

T (°C)	σ_y (MPa)	R_q (μm)	$\sigma_y R_q$ (N/mm)	Γ (J/m^2)	St Dev Γ (J/m^2)	# data pts
23	87	0.1	0.01	13.7	0.9	13
23	87	4	0.35	89.9	4.6	8
23	87	5	0.44	117.9	7.3	15
-25	140	4	0.56	126.8	4.4	10
-65	184	4	0.74	160.3	7.6	12

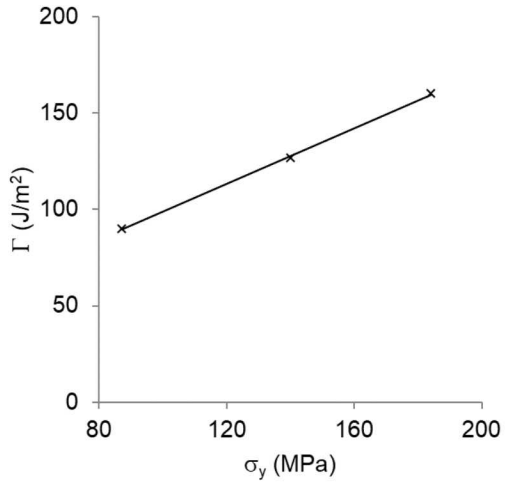

Figure 6. Measured aluminum/EPON 828/T403 epoxy interfacial toughness versus temperature dependent epoxy yield strength (R_q = 4 μm).

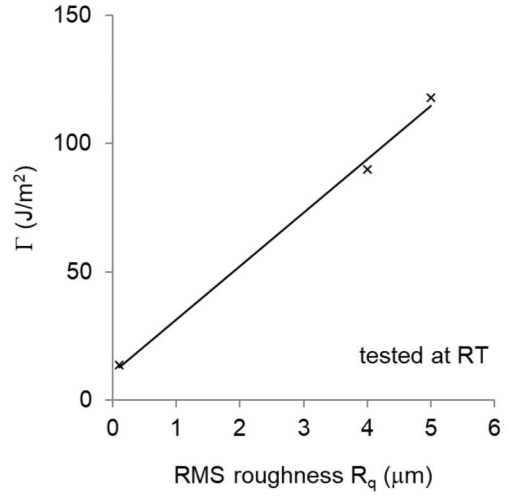

Figure 7. Measured aluminum/EPON 828/T403 epoxy interfacial toughness versus root mean square surface roughness R_q (T = 23 ºC).

3 Analysis

Here we define an illustrative problem to help explore possible connections between interfacial toughness, surface roughness, and polymer yield strength (which is linearly dependent on test temperature). First note that interfacial toughness data reported in this study are consistent with

small-scale crack-tip yielding (SSY). The plane strain crack-tip plastic zone size R_p for the case of a rigid adherend can be estimated in a way that is analogous to that commonly used for a crack in a homogeneous material (Tvergaard and Hutchinson 1993). Accordingly

$$R_p = \frac{1}{3\pi}\left[\frac{2\bar{E}\Gamma}{(1-\beta^2)\sigma_y^2}\right] \qquad \text{where} \qquad \beta = \frac{(1-2\nu)}{2(1-\nu)} \quad \text{and} \quad \bar{E} = \frac{E}{(1-\nu^2)} \tag{1}$$

where ν is the epoxy's Poisson's ratio (ν = 0.38), and E and σ_y are the temperature-dependent values listed in Table 1. Figure 8 plots the estimated values of R_p for the Epon828/DEA epoxy-to-aluminum interface toughness data (Table 2). Estimated R_p values are roughly commensurate with surface roughness R_q and these values are much smaller than the 500 μm ADCB bond thickness, etc. (i.e., SSY applies).

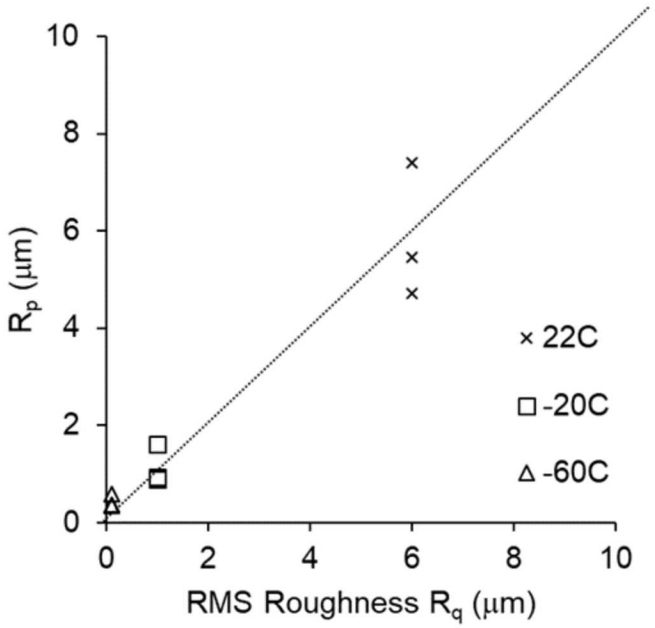

Figure 8. Estimated plastic zone size as a function of test temperature and surface roughness for the EPON 828/DEA epoxy-to-aluminum interface.

3.1 Illustrative model problem

Figure 9 shows the plane strain, small scale yielding problem that was analyzed. The goal was to identify as simple a problem as possible while still including all important variables. The upper material is rigid while the lower material is elastic-plastic. This is a reasonable approximation for aluminum/epoxy interfaces since all yielding is confined to the relatively low-stiffness epoxy. The loading is applied along the outer boundary where $r = R_o$ and is defined by the known linear elastic asymptotic crack-tip fields for a rigid/elastic interface (Rice, Suo et al. 1990). This applied loading defines the SSY analysis and the loading is specified in terms of an energy release rate G and crack-tip mode-mixity $\psi_{r=Ro}$. Elastic response is defined by elastic parameters E and ν. Crack-tip plastic yielding is defined by yield strength σ_y and other nondimensional parameters that depend on the choice of plasticity model (it is assumed that these parameters do not vary with σ_y). The model includes a crack-tip "bump" of radius a in front of a preexisting, initial interfacial crack. The bump radius a defines a characteristic length scale that reflects the magnitude of the surface roughness. More complex definitions of roughness could be defined using additional geometric parameters that are nondimensionalized by a.

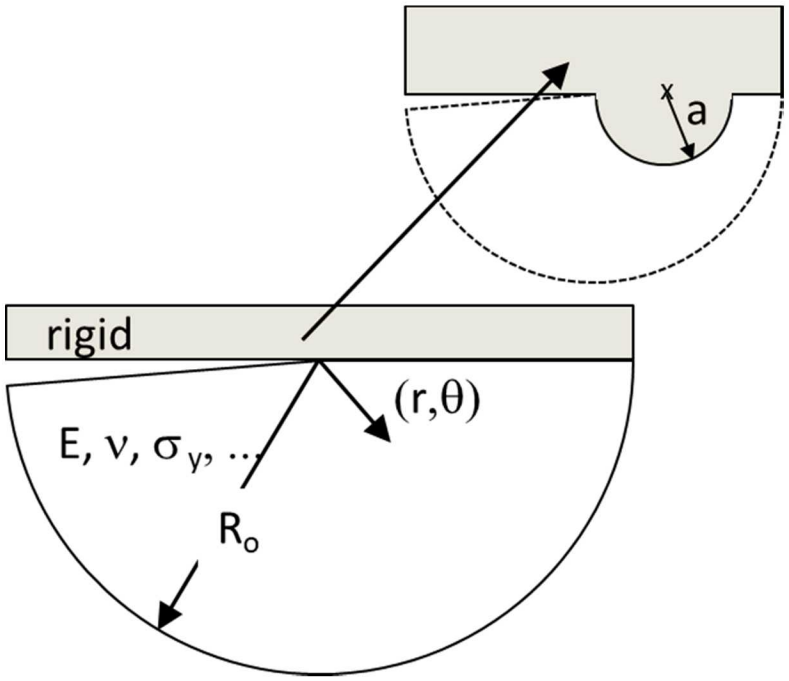

Figure 9. The plane strain, small scale yielding problem that was analyzed.

Here we desire a solution that determines strain $\hat{\varepsilon}$ at positions $(\hat{r}, \hat{\theta})$ that lie on the epoxy/bump interface in front of the interfacial crack.

3.2 Dimensional analysis

The problem defined in Fig. 9 depends on a small number of dimensional parameters. Based on dimensional considerations, strain $\hat{\varepsilon}$ on the epoxy/bump interface in front of the interfacial crack can be expressed as

$$\hat{\varepsilon} = f\left(\frac{\sigma_y}{E}, \frac{G}{\sigma_y a}, \frac{r}{a}, \theta, \psi_{r=R_o}, \nu, \ldots\right) \tag{2}$$

where σ_y and a are used as the primary dimensional parameters in the nondimensionalization.

We hypothesize that interfacial separation initiates once the plastic strain along the highly strained portion of the epoxy/bump interface exceeds the critical strain ε_h associated with rapid polymer hardening at large strains (e.g., in Fig. 3 when $\varepsilon > \approx 0.4$; a value that is independent of σ_y). This hypotheses is motivated by the coarse-grained molecular dynamics results published by Stevens (Stevens 2001); see the Introduction. We speculate that only after the epoxy chains are taut and the epoxy begins to rapidly harden at large strains can the chains can be pulled off the interface. By this time most of the available plastic dissipation has been used up.

In our ADCB tests, surface roughness and temperature-dependent yield strength was varied while the mode-mixity of the applied loading was fixed. To replicate this in the model problem, all model parameters are fixed with the exception of G, σ_y and a. Next consider the nondimensional relationship in Eq. 2. Under these conditions, strain at any fixed point along the epoxy/bump interface depends only on the first two nondimensional terms. Furthermore, if one assumes that within the zone of very large plastic strains at the epoxy/bump interface there is little dependence on the parameter σ_y/E then

$$\hat{\varepsilon} = f\left(\frac{G}{\sigma_y a}\right) \tag{3}$$

in the highly strained region adjacent to the epoxy/bump interface. The proposed criterion states that $G = \Gamma$ and the crack propagates when $\hat{\varepsilon} = \varepsilon_h$. Since ε_h is a constant and does not depend on σ_y

the criterion implies

$$\frac{\Gamma}{\sigma_y a} = a\ constant. \tag{4}$$

Consequently,

$$\Gamma \propto \sigma_y a. \tag{5}$$

This result suggests that the interfacial toughness measured during the ADCB tests scales as the product of the temperature-dependent epoxy yield strength and the magnitude of the surface roughness. Note that this result is similar to the crack-opening displacement δ_t vs. Γ relationship derived for small scale yielding using a Dugdale-Barenblatt strip yield zone model (Anderson 2005)

$$\Gamma \propto \sigma_y \delta_t. \tag{6}$$

A loose interpretation of the proposed scaling law (Eq. 5) is that the interfacial crack propagates at a critical COD that is commensurate with the magnitude of the roughness a.

3.3 Supporting finite element analysis

A limited number of finite element simulations was performed with the aim of validating the applicability of the scaling relationship that was suggested by a dimensional analysis (Eq. 5). The plane strain, small-scale yielding model problem shown in Fig. 9 was analyzed with model

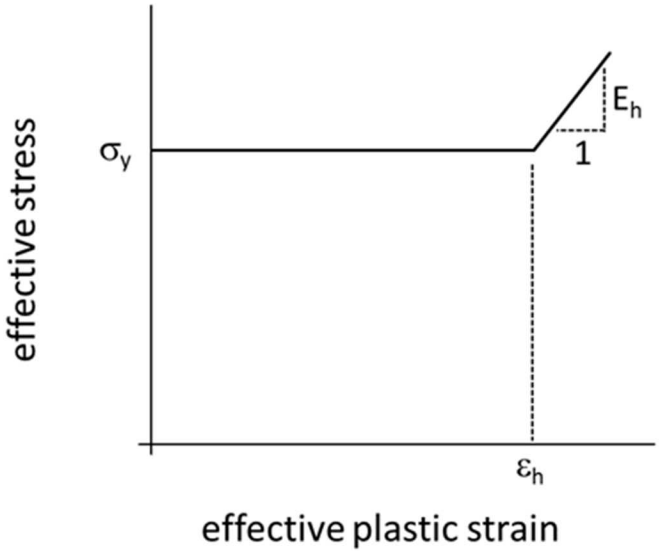

Figure 10. Effective stress-strain relationship used in finite element analysis.

parameters chosen to reflect our ADCB tests. A J2-plasticity model was used for the epoxy with an effective stress-strain relationship that is initially perfectly plastic-like but hardens at large strain (Fig. 10). This model does not include post-yield softening as observed in the tested epoxies since such models generate strain localization and mesh-dependent results that are difficult to interpret. This plasticity model does include extensive plastic dissipation prior to hardening at large strain. The model is defined by the parameters that are representative of the epoxies used in this study (E = 3 GPa, ν = 0.38, ε_h = 0.5, E_h = E/10, and σ_y = 90 or 180 MPa). In these small-scale yielding calculations, the asymptotic, far-field loading applied at $r = R_o$ = 1 mm generates a crack-tip mode-mixity $\psi_{r=Ro=1mm}$ = -30^o (this choice of ψ is similar to that of the ADCB specimens tested in this study). The prescribed energy release rate G was either 50 or 100 J/m^2 and the bump radius was either a = 0.005 or 0.010 mm (values consistent with the grit blasted surfaces). The mesh was highly refined in the region of the crack-tip bump, with a characteristic element length Δ of either 1e-4 or 2e-4 mm.

Figure 11 paints equivalent plastic strain contours for a = 0.005 mm, σ_y = 90 MPa, and G = 50 J/m^2. High equivalent plastic strain (with strains > 40%) is concentrated within a narrow band near the interface over a segment with $\omega < 60^o$ (see Fig. 11 for definition of ω). These results are for a

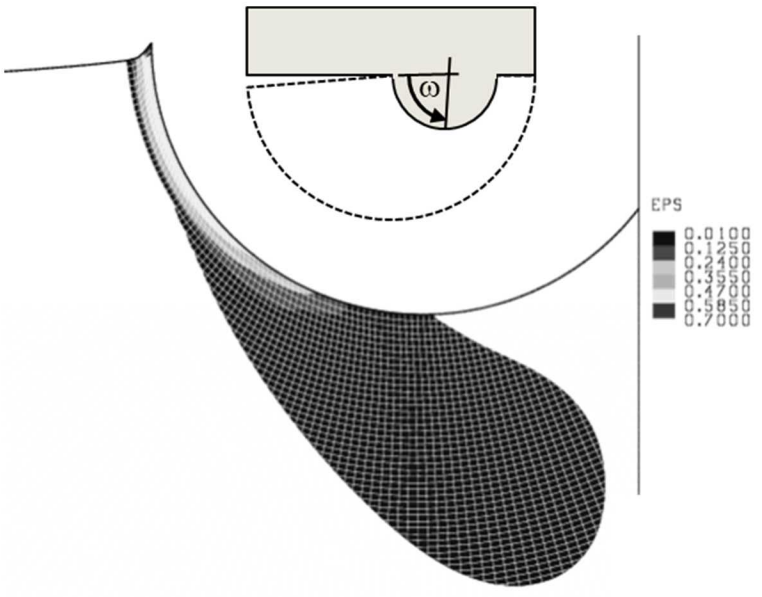

Figure 11. Equivalent plastic strain in region of bump at crack tip of the SSY model problem when a = 0.005 mm, σ_y = 90 MPa, and G = 50 J/m^2.

mesh with a characteristic element length Δ of 1e-4 mm in the highly refined region of the crack-tip bump. Calculations with a Δ of 2e-4 mm generate similar results. Figure 12 plots equivalent plastic strain adjacent to the interface vs. ω for the two values of Δ. There is good agreement in the calculated equivalent plastic strain at high strain levels with mesh refinement.

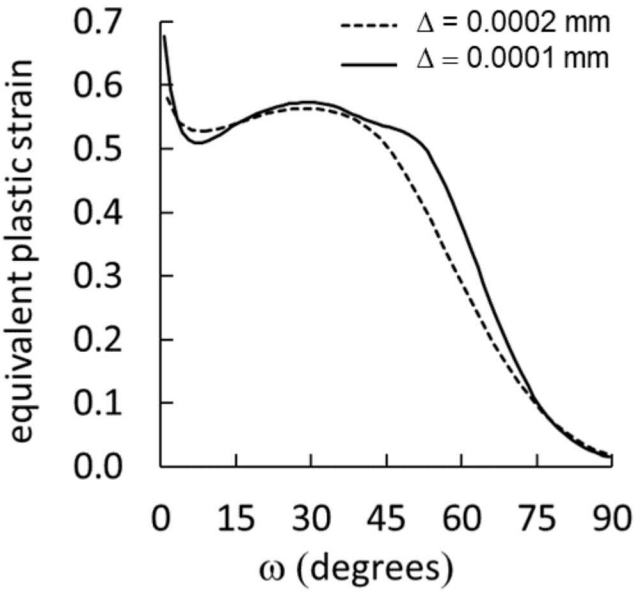

Figure 12. Equivalent plastic strain adjacent to the interface vs. ω for two values of characteristic mesh size Δ (a = 0.005 mm, σ_y = 90, G = 50 J/m^2).

The dimensional analysis suggests that for each ω, the plastic strain in the highly strained region adjacent to the epoxy/bump interface should remain unchanged when $\frac{G}{\sigma_y a}$ is held fixed (Eq. 3). In one test of this scaling relationship, results from three calculations with different values of σ_y and G are compared (a = 0.005 mm in all three calculations). Figure 13 shows that the two calculations with the same value of $\frac{G}{\sigma_y a}$ are in good agreement (in one case σ_y = 90, G = 50 J/m^2, while in the other σ_y = 180, G = 100 J/m^2). In contrast when the value of $\frac{G}{\sigma_y a}$ is cut in half (σ_y = 180, G = 50 J/m^2) the agreement is poor. In another test of this scaling, results from three calculations with

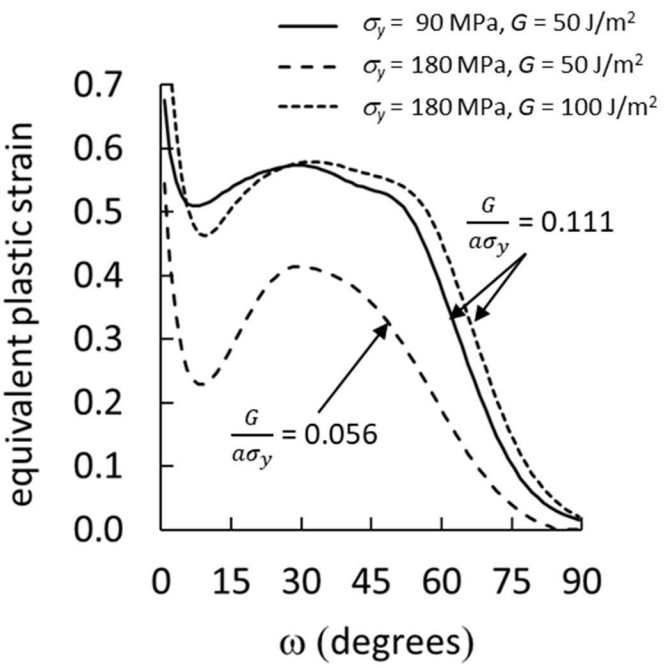

Figure 13. Equivalent plastic strain adjacent to the interface vs. ω for three different combinations of G and σ_y.

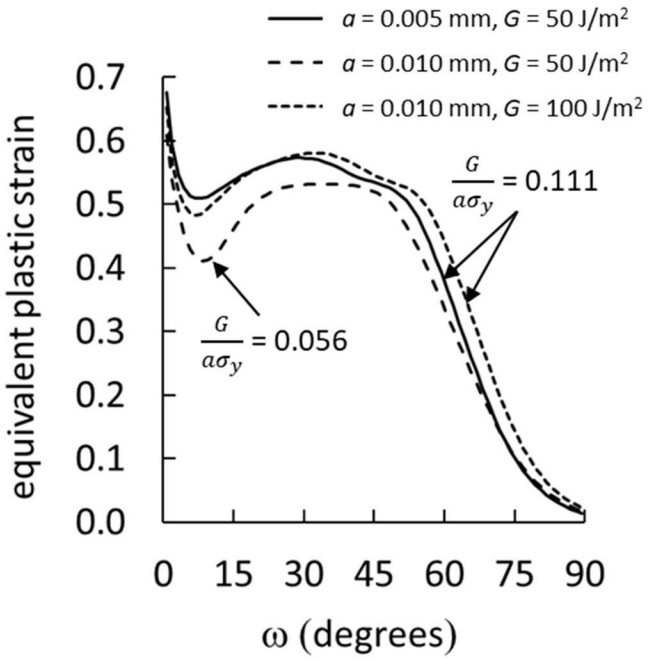

Figure 14. Equivalent plastic strain adjacent to the interface vs. ω for three different combinations of G and a.

different values of a and G are compared (σ_y = 90 in all three calculations). Figure 14 shows that the two calculations with the same value of $\frac{G}{\sigma_y a}$ are in good agreement (in one case a = 0.005 mm, G = 50 J/m^2, while in the other a = 0.010 mm, G = 100 J/m^2). In contrast when the value of $\frac{\Gamma}{\sigma_y a}$ is cut in half (a = 0.010 mm, G = 50 J/m^2) the agreement is poorer. These finite element results support to the proposed scaling relationship.

3.4 Comparison with experiment

The scaling relationship inferred from the dimensional analysis (Eq. 5), suggests that interface toughness scales as the product of the temperature dependent epoxy yield strength and a length scale that characterizes surface roughness. Accordingly, the ADCB toughness data measured in this study should be consistent with the relationship

$$\Gamma - \Gamma_o = C \sigma_y R_q. \qquad (7)$$

Here we replace a with the measure of surface roughness R_q used in our experiments. Furthermore, a constant Γ_o is added since at zero roughness there will be an intrinsic toughness associated with a perfectly smooth interface. Note that C is a constant (i.e., independent of σ_y and R_q) that depends on the specific nature of the epoxy/solid interface. For example, C could depend on how the interface was cleaned or what epoxy is used. The toughness data presented in Table 2 (EPON828/DEA epoxy) and Table 3 (EPON828/T403 epoxy) lists Γ and $\sigma_y R_q$ values for each temperature/surface roughness combination tested and this data is plotted in Fig. 15. Note that vertical bars associated with each toughness value indicates its 95% confidence interval on the measured mean value. As postulated, the data is consistent with a linear variation with respect to the compound parameter $\sigma_y R_q$. Both epoxy-to-aluminum interfaces display a linear variation, but both slope and intercept differ. Also shown on the plot is linear least squares fit for each epoxy-to-aluminum interface. This fit identifies the specific Γ_o and C values corresponding to the choice of epoxy adhesive.

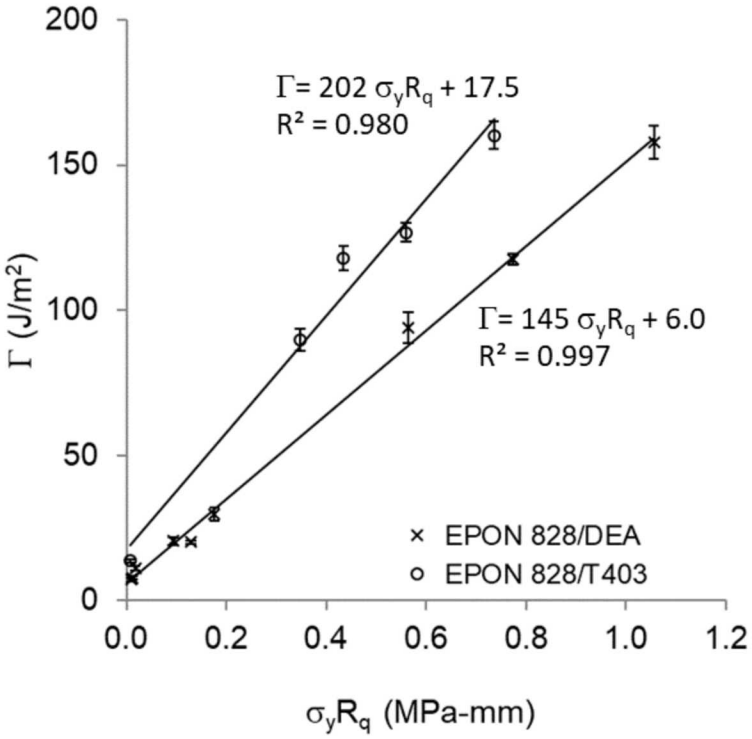

Figure 15. Measured interfacial toughness vs. the compound parameter $\sigma_y R_q$ for two different epoxy-to-aluminum interfaces (epoxy is either EPON828/DEA or EPON828/T403).

4 Conclusions

A simple relationship that connects interfacial toughness Γ, polymer yield strength σ_y (which is linearly dependent on test temperature), and interfacial surface roughness (here characterized by root mean square surface roughness R_q) has been identified. Specifically, Γ-$\Gamma_o = C\sigma_y R_q$ where Γ_o is associated with the interfacial toughness at zero roughness and C is a constant (i.e., independent of σ_y and R_q) that depends on the specific nature of the epoxy/solid interface. This relationship is perhaps surprising, connecting interfacial toughness to the product of two quantities that one might have otherwise assumed to be unrelated. One can envision performing tests that measure extremes in the (Γ, $\sigma_y R_q$) values of interest, and then using the linear fit to this data to estimate toughness over a broad range of test temperatures and surface roughness (of course, extrapolation outside of the measured (Γ, $\sigma_y R_q$) pairs is always risky).

The range of applicability of the proposed relationship has yet to be fully defined. This relationship is based upon dimensional considerations of a model problem that assumes that the characteristic length scale of both the roughness and the crack-tip yield zone is small relative to the region dominated by the linear elastic asymptotic crack-tip stress field. Furthermore, the polymer is assumed to rapidly harden at large strains. Potential limitations include cases where the interfacial toughness is significantly higher than the toughness of the polymer adhesive. In such cases, there could be a transition from interfacial to cohesive failure. Such a transition might occur as surface roughness is increased beyond some threshold value (since interfacial toughness increases with surface roughness). Furthermore, apparent interfacial toughness can increase rapidly with increasing crack-tip mode-mixity (i.e., when there is substantial crack-tip shear stress). Consequently, there could be a transition to cohesive failure as the applied crack-tip mode-mixity is increased above some threshold value. The proposed relationship is not expected to hold once cohesive failure dominates since one would no longer anticipate a strong dependence on surface roughness. It is also possible that the proposed relationship might be more broadly applicable than the cases addressed in this paper. For example, one might anticipate that interfacial toughness will depend on loading rate in a way that is similar to how it varies with temperature since increasing the loading rate in polymers is generally thought to be equivalent to decreasing the test temperature. There is a clear need for further work. Nonetheless, we anticipate the proposed relationship connecting interfacial toughness, surface roughness, and polymer yield strength is a starting point for reducing the amount of testing required to quantify the dependence of interfacial toughness on material and environmental conditions.

Acknowledgements

Sandia National Laboratories is a multimission laboratory managed and operated by National Technology and Engineering Solutions of Sandia, LLC., a wholly owned subsidiary of Honeywell International, Inc., for the U.S. Department of Energy's National Nuclear Security Administration under contract DE-NA-0003525. This paper describes objective technical results and analysis. Any subjective views or opinions that might be expressed in the paper do not necessarily represent the views of the U.S. Department of Energy or the United States Government.

References

Adolf, D. B., R. S. Chambers and J. M. Caruthers (2004). "Extensive Validation of a Thermodynamically Consistent, Nonlinear Viscoelastic Model for Glassy Polymers." Polymer **45**(13): 4599-4621.

Anderson, T. L. (2005). Fracture Mechanics: Fundamentals and Applications, CRC Press.

Bagheri, R., B. T. Marouf and R. A. Pearson (2009). "Rubber-Toughened Epoxies: A Critical Review." Polymer Reviews **49**(3): 201-225.

Bao, G., S. Ho, Z. Suo and B. Fan (1992). "The Role of Material Orthotropy in Fracture Specimens for Composites." International Journal of Solids and Structures **29**: 1105-1116.

Brown, H. R. (1990). "Mixed-Mode Effects on the Toughness of Polymer Interfaces." Journal of Materials Science **25**(6): 2791-2794.

Buckley, C. P., J. Harding, J. P. Hou, C. Ruiz and A. Trojanowski (2001). "Deformation of Thermosetting Resins at Impact Rates of Strain. Part I: Experimental Study." Journal of the Mechanics and Physics of Solids **49**: 1517-1538.

Hutchinson, J. W. and Z. Suo (1992). Mixed Mode Cracking in Layered Materials. Advances in Applied Mechanics. J. W. Hutchinson and T. Y. Wu, Academic Press. **29:** 63-191.

Jennings, C. W. (1972). "Surface-Roughness and Bond Strength of Adhesives." Journal of Adhesion **4**(1): 25-38.

Kinloch, A. J. (1980). "The Science of Adhesion .1. Surface and Interfacial Aspects." Journal of Materials Science **15**(9): 2141-2166.

Kinloch, A. J. (1982). "The Science of Adhesion .2. Mechanics and Mechanisms of Failure." Journal of Materials Science **17**(3): 617-651.

McClintock, F. A. and A. S. Argon (1966). Mechanical Behavior of Materials, Addison-Wesley Pub. Co.

Packham, D. E. (2003). "Surface Energy, Surface Topography and Adhesion." International Journal of Adhesion and Adhesives **23**: 437-448.

Pocius, A. V. (1997). Adhesion and Adhesives Technology. Cincinnati, Hanser Gardner Publications, Inc.

Reedy, E. D., Jr. and T. R. Guess (1993). "Comparison of Butt Tensile Strength Data with Interface Corner Stress Intensity Factor Prediction." International Journal of Solids and

Structures **30**: 2929-2936.

Reedy, E. D., Jr. and T. R. Guess (1995). "Butt Joint Tensile Strength: Interface Corner Stress Intensity Factor Prediction." Journal of Adhesion Science and Technology **9**: 237-251.

Reedy, E. D., Jr. and T. R. Guess (1999). "Additional Interface Corner Toughness Data for an Adhesively-Bonded Butt Joint." International Journal of Fracture **98**: L3-L8.

Rice, J. R., Z. Suo and J. S. Wang (1990). Mechanics and Thermodynamics of Brittle Interfacial Failure in Bimaterial Systems. Metal-Ceramic Interfaces. M. Ruhle, A. G. Evans, M. F. Ashby and J. P. Hirth. New York, Pergamon Press**:** 269-294.

Rider, A. N. and D. R. Arnott (2001). "The Influence of Adherend Topography on the Fracture Toughness of Aluminum-Epoxy Adhesive Joints in Humid Environments." Journal of Adhesion **75**: 203-228.

Shahid, M. and S. A. Hashim (2002). "Effect of Surface Roughness on the Strength of Cleavage Joints." International Journal of Adhesion and Adhesives **22**(3): 235-244.

Stevens, M. J. (2001). "Interfacial Fracture between Highly Cross-linked Polymer Networks and a Solid Surface: Effect of Interfacial Bond Density." Macromolecules **34**(8): 2710-2718.

Suo, Z. and J. W. Hutchinson (1989). "Sandwich Test Specimens for Measuring Interface Crack Toughness." Materials Science and Engineering **A107**: 135-143.

Tvergaard, V. and J. W. Hutchinson (1993). "The influence of plasticity on mixed mode interface toughness." Journal of the Mechanics and Physics of Solids **41**: 1119-1135.

Volinsky, A. A., N. R. Moody and W. W. Gerberich (2002). "Interfacial toughness measurements for thin films on substrates." Acta Materialia **50**(3): 441-466.

Zhang, S., R. Panat and K. J. Hsia (2003). "Influence of Surface Morphology on the Adhesion Strength of Epoxy-Aluminum Interfaces." Journal of Adhesion Science and Technology **17**: 1685-1711.

Zhang, Y. L. and G. M. Spinks (1997). "An Atomic Force Microscopy Study of the Effect of Surface Roughness on the Fracture Energy of Adhesively Bonded Aluminium." Journal of Adhesion Science and Technology **11**(2): 207-223.